Available online at www.sciencedirect.com
SCIENCE DIRECT®
Chemical Physics Letters 375 (2003) 445–451
CHEMICAL PHYSICS LETTERS
www.elsevier.com/locate/cplett

Structural, electronic, and magnetic properties of heterofullerene $C_{48}B_{12}$

Rui-Hua Xie [a,*], Lasse Jensen [b], Garnett W. Bryant [a], Jijun Zhao [c], Vedene H. Smith Jr. [d]

[a] National Institute of Standards and Technology, Gaithersburg, MD 20899-8423, USA
[b] Theoretical Chemistry, Materials Science Centre, Rijksuniversiteit Groningen, Nijenborgh 4, 9747 AG Groningen, The Netherlands
[c] Department of Physics and Astronomy, University of North Carolina, Chapel Hill, NC 27599, USA
[d] Department of Chemistry, Queen's University, Kingston, Ont., Canada K7L 3N6

Received 12 March 2003; in final form 1 May 2003

Abstract

Bonding, electric (hyper)polarizability, vibrational, and magnetic properties of heterofullerene $C_{48}B_{12}$ are studied by first-principles calculations. Infrared- and Raman-active vibrational frequencies of $C_{48}B_{12}$ are assigned. Eight ^{13}C and two ^{11}B nuclear magnetic resonance (NMR) spectral signals of $C_{48}B_{12}$ are characterized. The average second hyperpolarizability of $C_{48}B_{12}$ is about 180% larger than that of C_{60}. Our results suggest that $C_{48}B_{12}$ is a candidate for photonic and optical limiting applications because of the enhanced third-order optical non-linearities.

1. Introduction

In 1985, Kroto et al. [1] proposed the existence of C_{60} clusters in their graphite laser vaporization experiment. This proposal was subsequently confirmed in 1990 when Krätschmer et al. [2] reported a method for the mass production of C_{60} in a carbon arc along with infrared (IR) spectroscopic evidence for the C_{60} carbon structure. These pioneering works have stimulated extensive research into fullerenes [3,4], a new form of pure carbon, where an even number of three-coordinated sp^2 carbon atoms arrange themselves into 12 pentagonal faces and any number (>1) of hexagonal faces. These carbon-cage molecules can crystallize into a variety of three-dimensional structures [2] and be doped in several different ways [4]: endohedral doping, where the dopant is inside the fullerene cage; substitutional doping, where the dopant is on the fullerene cage; and exohedral doping, where the dopant is outside or between fullerene cages. It has been shown that doped fullerenes have remarkable structural, electronic, optical, and magnetic properties [4–6].

In 1995, the heterofullerene $C_{59}N$ was formed efficiently in the gas phase during fast atom

* Corresponding author. Fax: 1-301-990-1350.
E-mail address: rhxie@nist.gov (R.-H. Xie).

0009-2614/03/$ - see front matter © 2003 Elsevier Science B.V. All rights reserved.
doi:10.1016/S0009-2614(03)00879-0

bombardment mass spectroscopy of a cluster-opened *N*-methoxyethoxy methyl ketolactam [7]. The isolation and characterization of biazafullerenyl has opened a viable route for the preparation of $C_{59}N$ and other heterofullerenes in solution, leading to a number of detailed theoretical and experimental studies of $C_{59}N$ and heterofullerenes [4–6]. In 1991, the Smalley group [8] successfully synthesized boron-substituted fullerenes $C_{60-n}B_n$ ($1 \leqslant n \leqslant 6$). Very recently, Hultman et al. [9] have successfully synthesized aza-fullerenes $C_{60-n}N_n$, formed by substituting carbon atoms in C_{60} with more than one nitrogen atom, and the existence of a stable $C_{48}N_{12}$ aza-fullerene [9–12] was revealed. Stimulated by the high stability of $C_{48}N_{12}$, we have recently predicted that $C_{48}B_{12}$ [13] is also a stable heterofullerene and can be a promising component for molecular rectifiers, nanotube-based transistors, and p–n junctions.

In this Letter, we further study the bonding, Mulliken charges, electric (hyper)polarizability, vibrational, and magnetic properties of $C_{48}B_{12}$. We characterize ^{13}C and ^{11}B NMR spectral lines of $C_{48}B_{12}$ and show how the boron-substitutional doping modifies the IR and Raman spectra of the pristine C_{60}. We also find that $C_{48}B_{12}$ exhibits enhanced second hyperpolarizability (enhanced third-order optical non-linearity) and can compete with C_{60} and aza-fullerene $C_{48}N_{12}$ as a candidate for photonic and optical limiting applications (for example, data processing, eye and sensor protection, all-optical switching, and optical limiting) [6].

2. Bonding and Mulliken charge

The geometry of $C_{48}B_{12}$, shown in Fig. 1, was fully optimized by using the GAUSSIAN 98 program [1] [14]. We have used the B3LYP [15] hybrid density functional theory (DFT) method, which includes a mixture of Hartree–Fock (exact) exchange, Slater local exchange [16], Becke 88 non-local exchange [17], the VWN III local exchange-correlation functional [18] and the LYP correlation functional [19], and a 6-31G(d) basis set. The dopant assignment of $C_{48}B_{12}$ considered is illustrated in Fig. 1: each pentagon has one boron atom and two boron atoms preferentially sit in one hexagon. The symmetry of $C_{48}B_{12}$ is found to be a C_i point group. The distances (or radii) R_i from the ith atom to the density center of the molecule are listed in Table 1. We find that $C_{48}B_{12}$, similar to $C_{48}N_{12}$ [11], is an ellipsoid structure with 10 unique radii, while C_{60} has the same radius for each carbon atom (calculated $R_i = 0.35502$ nm, in excellent agreement with experiment [20]).

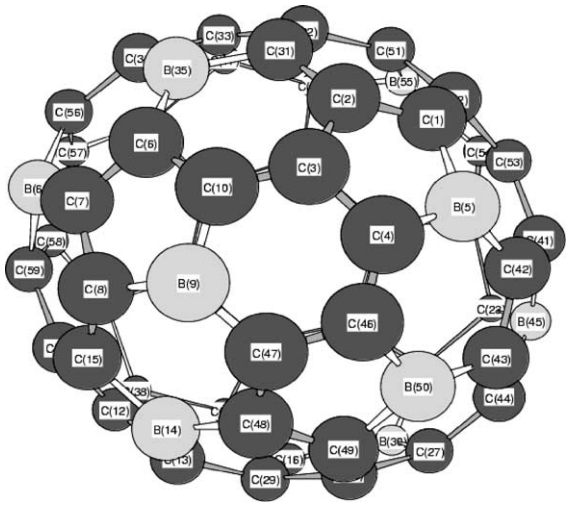

Fig. 1. $C_{48}B_{12}$ geometric structure optimized with B3LYP/6-31G(d). The site numbers {5, 9, 14, 21, 26, 30, 35, 39, 45, 50, 55, 60} are for boron atoms and the others for carbon atoms.

The calculated net Mulliken charges Q_i of carbon and boron atoms in $C_{48}B_{12}$ are listed in Table 1. Like $C_{48}N_{12}$ [10,11], the heterofullerene $C_{48}B_{12}$ has two types of boron dopants in the structure: one with net Mulliken charges $Q_i = 0.1637e$ and the other with $Q_i = 0.1871e$. All carbon atoms in $C_{48}B_{12}$ have negative Q_i. Although the Mulliken analysis cannot predict exactly the atomic charges quantitatively, the sign of atomic charge is correct [21]. From the Mulliken analysis, we see that boron atoms in $C_{48}B_{12}$ exist as electron donor while carbon atoms act as electron acceptors. The calculated charge of boron atom is consistent with the experimental result of the Smalley group [8] that

[1] Use of this software does not constitute an endorsement or certification by NIST.

Table 1
B3LYP/6-31G(d) calculations of radius (R_i, in nm) and net Mulliken charge (Q_i, in e, where 1 $e = 1.6 \times 10^{-19}$ C) for $C_{48}B_{12}$

Site number $\{n_i\}$	Atom	R_i	Q_i
{1, 13, 16, 31, 38, 51}	C	0.35198	−0.0385
{2, 12, 29, 32, 37, 52}	C	0.34652	−0.0079
{3, 11, 28, 33, 36, 53}	C	0.35701	−0.0036
{4, 15, 27, 34, 40, 54}	C	0.37033	−0.0712
{5, 14, 30, 35, 39, 55}	B	0.36454	0.1637
{6, 18, 24, 42, 48, 58}	C	0.37116	−0.0333
{7, 19, 23, 43, 47, 57}	C	0.38035	−0.0376
{8, 20, 22, 44, 46, 56}	C	0.38252	−0.0826
{9, 21, 26, 45, 50, 60}	B	0.37953	0.1871
{10, 17, 25, 41, 49, 59}	C	0.37079	−0.0761

Table 2
B3LYP/6-31G(d) calculation of CC and BC bond lengths (nm) in molecule $C_{48}B_{12}$

Bond	Site number pairs for bonding	Bond length
CC	(1, 2) (12, 13) (16, 29) (31, 32) (37, 38) (51, 52)	0.14261
BC	(1, 5) (13, 14) (16, 30) (31, 35) (38, 39) (51, 55)	0.15376
CC	(1, 52) (2, 31) (12, 38) (13, 29) (16, 37) (32, 51)	0.14078
CC	(2, 3) (11, 12) (28, 29) (32, 33) (36, 37) (52, 53)	0.15014
CC	(3, 4) (11, 15) (27, 28) (33, 34) (36, 40) (53, 54)	0.14871
CC	(3, 10) (11, 59) (17, 33) (25, 36) (28, 49) (41, 53)	0.13861
BC	(4, 5) (14, 15) (27, 30) (39, 40) (34, 35) (54, 55)	0.15667
CC	(4, 46) (8, 15) (20, 40) (22, 54) (27, 44) (34, 56)	0.13867
BC	(5, 42) (6, 35) (14, 48) (18, 55) (24, 30) (39, 58)	0.15576
CC	(6, 10) (17, 18) (24, 25) (58, 59) (41, 42) (48, 49)	0.14682
CC	(6, 7) (18, 19) (23, 24) (42, 43) (47, 48) (57, 58)	0.14080
BC	(7, 60) (9, 47) (19, 26) (21, 57) (23, 45) (43, 50)	0.15594
CC	(7, 8) (19, 20) (22, 23) (43, 44) (46, 47) (56, 57)	0.14570
BC	(8, 9) (20, 21) (22, 26) (44, 45) (46, 50) (56, 60)	0.15899
BC	(9, 10) (17, 21) (25, 26) (41, 45) (49, 50) (59, 60)	0.15563

an electron-deficient site was produced at the boron position on the cage.

The optimized carbon–carbon (CC) and boron–carbon (BC) bond lengths in $C_{48}B_{12}$ are listed in Table 2. We find that $C_{48}B_{12}$ has six unique BC bond lengths in the range of 0.15376–0.15899 nm and nine unique CC bond lengths in the range of 0.13861–0.15014 nm. For C_{60} molecule, the double C=C bond and single C–C bond lengths are 0.13949 and 0.14539 nm, respectively, in excellent agreement with experiment [20].

3. Electric (hyper)polarizability

The static dipole polarizability (SDP) for heterofullerene $C_{48}B_{12}$ is presented in Table 3. The B3LYP results were obtained by using the GAUSSIAN 98 program [1] [14], while the local density approximation (LDA) results were calculated by using the Amsterdam Density Functional (ADF) program [1] [22,23]. The SDPs for $C_{48}N_{12}$ and C_{60} listed in Table 3 are taken from our recent work [24]. For the B3LYP calculations, we use the valence-split basis set 6-31G(d) including the polarization functions for boron and carbon atoms. The ADF program uses basis sets of Slater functions. In this work, we use a triple zeta valence plus polarization (TZP) augmented with field-induced polarization (FIP) functions of Zeiss et al. [25]. This basis set, TZP++ ([6s4p2d1f] for carbon and boron atoms), was previously used for calculating the second hyperpolarizability γ of C_{60} and its derivatives (for example, $C_{58}N_2$, $C_{58}B_2$, and

Table 3
Static dipole polarizability (α, in nm^3) for $C_{48}B_{12}$, $C_{48}N_{12}$ and C_{60} calculated with B3LYP/6-31G(d), and LDA/TZP++

Molecule	B3LYP/6-31G(d)		LDA/TZP++		Ref.
	α_{xx}	α_{zz}	α_{xx}	α_{zz}	
C_{60}	0.0695	0.0695	0.0847	0.0847	[24]
$C_{48}N_{12}$	0.0666	0.0675	0.0793	0.0815	[24]
$C_{48}B_{12}$	0.0822	0.0804	0.0958	0.0939	This work

The symmetry relation for C_{60} gives $\alpha_{xx} = \alpha_{yy} = \alpha_{zz}$ and for $C_{48}B_{12}$ and $C_{48}N_{12}$ is $\alpha_{xx} = \alpha_{yy}$.

Table 4
The static second hyperpolarizabilities (γ, in a.u., with 1 a.u. $= 6.235378 \times 10^{-65}$ C^4 m^4 J^{-3}) for $C_{48}B_{12}$, $C_{48}N_{12}$, and C_{60} calculated by using LDA and a TZP++ basis set

Molecule	γ_{xxxx}	γ_{xxyy}	γ_{zzzz}	γ_{xxzz}	γ_{zzxx}	$\overline{\gamma}$	Ref.
C_{60}	137 950	45 983	137 950	45 983	45 983	137 950	[24]
$C_{48}N_{12}$	188 780	62 880	232 970	85 120	84 790	215 222	[24]
$C_{48}B_{12}$	470 190	156 840	214 300	116 800	118 090	387 628	This work

The average second hyperpolarizability is given by $\overline{\gamma} = \frac{1}{15}\sum_{i,j}(\gamma_{iijj} + \gamma_{ijij} + \gamma_{ijji})$. The symmetry relations of the molecule gives $\gamma_{xxxx} = \gamma_{yyyy}$, $\gamma_{xxzz} = \gamma_{yyzz}$, and $\gamma_{zzxx} = \gamma_{zzyy}$.

$C_{58}BN$) and has been shown to produce reasonable (hyper)polarizabilities even with its small size [26]. Here, we only make a comparison between $C_{48}B_{12}$, $C_{48}N_{12}$, and C_{60}. A comparison of C_{60} with other theoretical and experimental results can be found in review chapters [5,6] and recent work [24,26].

From Table 3, we see that the LDA results are about 20% larger than the corresponding B3LYP ones. This is expected since the basis set in the LDA calculation is larger and the LDA method, in general, predicts a larger polarizability than the B3LYP method [27]. Nevertheless, both B3LYP and LDA predict the same trends. The mean polarizability of $C_{48}B_{12}$ in the LDA (B3LYP) is about 12% (15%) larger than that of C_{60}.

The first hyperpolarizability β of $C_{48}B_{12}$ is zero due to inversion symmetry. The static second hyperpolarizability, γ, for $C_{48}B_{12}$, $C_{48}N_{12}$, and C_{60} are presented in Table 4. The γ values for $C_{48}N_{12}$ and C_{60} listed in Table 4 are taken from [24], and the comparison will only be made between these three molecules. For the calculations of the second hyperpolarizability, we use time-dependent DFT (TD-DFT) method as described in [26,28], i.e., finite-field differentiation of the analytically calculated first hyperpolarizability. For all TD-DFT calculations, we used the RESPONSE code [1] [29] implemented in the ADF program [1] [22,23].

We find for all components of the second hyperpolarizability for both $C_{48}B_{12}$ and $C_{48}N_{12}$ a larger value than for C_{60}. All γ components for $C_{48}B_{12}$ are also larger than the corresponding components for $C_{48}N_{12}$ except for the γ_{zzzz}. This gives an average second hyperpolarizability, $\overline{\gamma}$ of $C_{48}B_{12}$, which is about 180% larger than that of C_{60}. In contrast, the $\overline{\gamma}$ value for $C_{48}N_{12}$ is about 55% larger than that of C_{60}. The increase in the second hyperpolarizability is much larger for $C_{48}B_{12}$ than for $C_{48}N_{12}$ especially considering that there is no increase in volume. It has been experimentally shown that C_{60} is a good optical limiter [6] because of its larger γ value. Our present results imply that heterofullerene $C_{48}B_{12}$ can compete with C_{60} as an even better optical limiter because of its enhanced third-order optical non-linearity.

4. IR and Raman spectra

Using the GAUSSIAN 98 program [1] [14], we first optimize the geometry of $C_{48}B_{12}$ and C_{60} with the B3LYP method and 3-21G basis set. Then, we calculate the vibrational frequencies of $C_{48}B_{12}$ and

C_{60} with the same method and basis set. Our results for C_{60} are in agreement with experiment [30,31]. C_{60} has totally 46 vibrational modes [4]. Since $C_{48}B_{12}$ has lower symmetry (C_i) than C_{60}, we find 174 independent vibrational modes for $C_{48}B_{12}$: 87 non-degenerate IR-active modes with a_u symmetry and 87 non-degenerate Raman-active modes with a_g symmetry.

We also calculate IR intensities I_{IR} and Raman scattering activities Ω_{Raman} at the corresponding vibrational frequencies for both C_{60} and heterofullerene $C_{48}B_{12}$. The results are shown in Figs. 2 and 3. Since experimental IR and Raman spectroscopic data do not directly indicate the specific type of nuclear motion producing each spectroscopic peak, we do not give here the normal mode displacement for the vibrational frequencies.

For C_{60}, we note that its IR spectrum is very simple. Namely, it is composed of four IR spectroscopic signals with t_{1u} symmetry. The IR intensities for C_{60} calculated with B3LYP/3-2G agree reasonably with the in situ high-resolution FTIR spectrum of a C_{60} film measured by Onoe and Takeuchi [32]. However, the IR spectrum of $C_{48}B_{12}$ is not so simple, exhibiting 87 IR spectroscopic signals, with the stronger IR spectroscopic signals mainly in the high-frequency region. Here

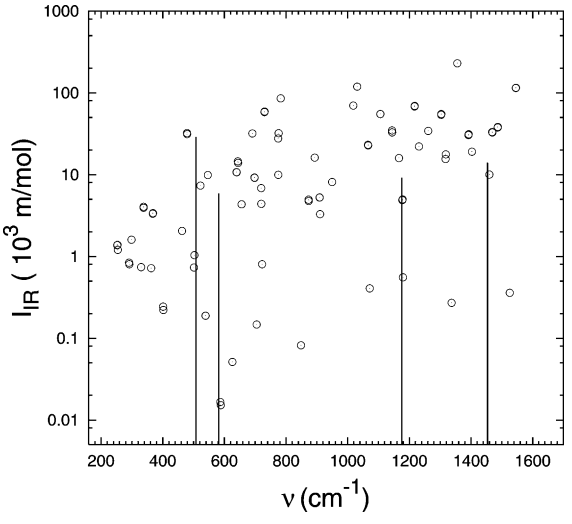

Fig. 2. B3LYP/3-21G calculation of IR-active vibrational frequencies (v, in cm^{-1}) and IR intensities (I_{IR}, in 10^3 m/mol) of $C_{48}B_{12}$ (open circles) and C_{60} (solid lines).

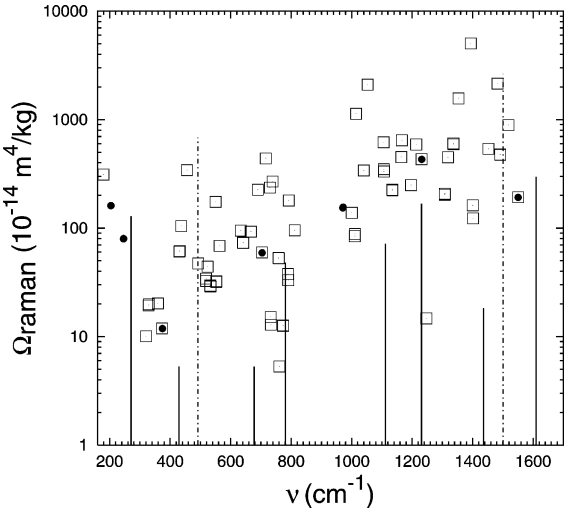

Fig. 3. B3LYP/3-21G calculations of Raman-active frequencies (v, in cm^{-1}) and Raman scattering activities (Ω_{Raman}, in 10^{-14} m^4/kg) of $C_{48}B_{12}$. The solid and dot-dashed lines are the unpolarized and polarized Raman spectral lines of C_{60}, respectively. Filled circles and open squares are non-degenerate unpolarized and polarized Raman-active modes, respectively.

we discuss several vibrational bands in the IR intensity of $C_{48}B_{12}$ to be compared with future experimental identification: (i) the strongest IR spectroscopic signal with IR intensity of 229 912 m/mol is determined at the high frequency 1356 cm^{-1}; (ii) three strong modes are observed at frequencies $v = 783$, 1031, and 1546 cm^{-1} with IR intensities of 85 828, 119 322, and 114 878 m/mol, respectively; (iii) five intermediate modes appear at frequencies $v = 730$, 1018, 1106, 1217, and 1303 cm^{-1} with IR intensities of 58 303, 69 950, 55 094, 69 160, and 53 856 m/mol, respectively.

As shown in Fig. 3, C_{60} has two non-degenerate polarized Raman spectroscopic signals with a_g symmetry and eight fivefold-degenerate unpolarized ones with h_g symmetry. The strongest Raman spectroscopic signals in C_{60} are the two a_g modes. The calculated results for C_{60} are in excellent agreement with experiment [31]. In contrast, for $C_{48}B_{12}$, we observe 10 non-degenerate unpolarized and 77 non-degenerate polarized Raman spectroscopic signals with a_g symmetry. The Raman spectrum separates into high-frequency (1000–1700 cm^{-1}) and low-frequency (200–900 cm^{-1})

regions, similar to those of C_{60}. The strong Raman spectroscopic signals in $C_{48}B_{12}$ are the non-degenerate polarized modes. Three strong Raman bands of $C_{48}B_{12}$ are: (i) the strongest Raman spectroscopic signal in $C_{48}B_{12}$ appears at high frequency $\nu = 1394$ cm^{-1} with $\Omega_{\text{Raman}} = 5035 \times 10^{-14}$ m^4/kg; (ii) four strong Raman spectroscopic signals are located at $\nu = 1014$, 1053, 1353, and 1482 cm^{-1} with $\Omega_{\text{Raman}} = 1130 \times 10^{-14}$, 2094×10^{-14}, 1568×10^{-14}, and 2149×10^{-14} m^4/kg, respectively; (iii) five intermediate strong Raman spectroscopic signals are observed at $\nu = 1105$, 1166, 1214, 1336, and 1518 cm^{-1} with $\Omega_{\text{Raman}} = 618 \times 10^{-14}$, 644×10^{-14}, 590×10^{-14}, 601×10^{-14}, 537×10^{-14}, and 887×10^{-14} m^4/kg, respectively.

5. Second-order magnetic response

There are a number of theoretical methods for calculating the second-order magnetic response properties of molecules. In this Letter, we use both the gauge-including-atomic-orbital (GIAO) method and the continuous-set-of-gauge-transformation (CSGT) procedure [33], which is implemented in the GAUSSIAN 98 program [1] [14], to predict the NMR shielding tensors σ of $C_{48}B_{12}$. In high-resolution NMR, the isotropic part σ_{iso} of σ is measured by taking the average of σ with respect to the orientation to the magnetic field, i.e., $\sigma_{\text{iso}} = (\sigma_{xx} + \sigma_{yy} + \sigma_{zz})/3$, where σ_{xx}, σ_{yy}, and σ_{zz} are the principal axis values of σ. The results calculated by using B3LYP hybrid DFT and restricted Hartree–Fock (RHF) theory are summarized in Table 5. We find that $C_{48}B_{12}$ has eight ^{13}C and two ^{11}B NMR spectral signals, indicative of the 10 unique sites in the $C_{48}B_{12}$ structure. In contrast, C_{60} has only one ^{13}C NMR spectral signal, for example, with $\sigma_{\text{iso}} = 50.5$ ppm (parts per million) and 54.7 ppm obtained with B3LYP/6-31G(d):GIAO and RHF/6-31G(d):GIAO, respectively. The ^{13}C NMR chemical shift ($\delta = \sigma_{\text{iso}}^{\text{TMS}} - \sigma_{\text{iso}}^{\text{sample}}$) with respect to the reference tetramethysilane (TMS) for C_{60} is, for example, $\delta = 133.3$ (135.7) ppm for B3LYP/6-31G(d):GIAO (B3LYP/6-31G(d):CSGT), about 9 (7) ppm difference from experiment ($\delta = 142.7$ ppm, [34]), but $\delta = 140.4$ (141.7) ppm for RHF/6-31G(d):GIAO (RHF/6-31G(d):CSGT) which is in good agreement with experiment. The results for C_{60} show that the DFT method does not provide systematically better NMR results than RHF. This is due to the fact that no current functionals include a magnetic field dependence [33]. For C_{60}, the CSGT procedure provides better NMR results than the GIAO procedure when compared to experiment, but takes more CPU time (see Table 5) than the GIAO procedure.

6. Summary

In summary, we have performed first-principles calculations of bonding, Mulliken charges, dipole polarizability, hyperpolarizability, vibrational frequencies, IR intensities, Raman scattering activities, and second-order magnetic response properties of heterofullerene $C_{48}B_{12}$. Eighty-seven independent IR-active and 87 independent Raman-active vibrational modes for $C_{48}B_{12}$ are

Table 5
B3LYP/6-31G(d) and RHF/6-31G(d) calculations of the absolute isotropy, σ_{iso} in ppm (parts per million), of the nuclear magnetic shielding tensor σ for atoms in $C_{48}B_{12}$, C_{60}, and tetramethysilane (TMS) found by using both GIAO and CSGT methods

Theoretical method	$C_{48}B_{12}$										TMS	C_{60}	
	^{13}C[1]	^{13}C[2]	^{13}C[3]	^{13}C[4]	^{11}B[5]	^{13}C[6]	^{13}C[7]	^{13}C[8]	^{11}B [9]	^{13}C[10]	^{13}C	^{13}C	CPU
B3LYP/6-31G(d):GIAO	42.9	19.1	25.6	27.4	65.2	2.7	17.1	32.3	73.6	37.6	183.8	50.5	26.6
B3LYP/6-31G(d):CSGT	39.3	16.0	21.9	23.7	60.3	0.8	13.9	28.8	69.1	34.0	181.6	45.9	28.5
RHF/6-31G(d):GIAO	59.7	21.2	41.4	52.2	73.1	24.6	36.8	37.2	75.2	56.4	195.1	54.7	13.5
RHF/6-31G(d):CSGT	55.0	17.5	36.9	47.1	68.4	20.8	31.7	33.0	71.0	51.9	190.6	48.9	18.5

The CPU times (h) for C_{60} cases are shown.

assigned. Eight ^{13}C and two ^{11}B NMR spectral lines for $C_{48}B_{12}$ are characterized. Compared to C_{60} and $C_{48}N_{12}$, $C_{48}B_{12}$ exhibits enhanced third-order optical non-linearity, which implies potential applications of $C_{48}B_{12}$ in photonics and optical limiting.

Acknowledgements

We thank Dr. Denis A. Lehane and Dr. Hartmut Schmider for their technical help. One of us (R.H.X.) thanks the HPCVL at Queen's University for the use of its parallel supercomputing facilities. L.J. gratefully acknowledges the Danish Research Training Council for financial support. V.H.S. acknowledges support from the Natural Science and Engineering Research Council of Canada (NSERC).

References

[1] H.W. Kroto, J.R. Heath, S.C. O'Brien, R.E. Curl, R.E. Smalley, Nature (London) 318 (1985) 162.
[2] W. Krätschmer, L.D. Lamb, K. Fostiropoulos, D.R. Huffman, Nature (London) 347 (1990) 354.
[3] H.W. Kroto, J.E. Fischer, D.E. Cox, The Fullerenes, Pergamon, Oxford, 1993.
[4] M.S. Dresselhaus, G. Dresselhaus, P.C. Eklund, Science of Fullerenes and Carbon Nanotubes, Academic Press, New York, 1996.
[5] R.H. Xie, in: H.S. Nalwa (Ed.), Handbook of Advanced Electronic and Photonic Materials and Devices, Nonlinear Optical Materials, vol. 9, Academic Press, New York, 2000, pp. 267–307 (Chapter 6).
[6] R.H. Xie, Q. Rao, L. Jensen, in: H.S. Nalwa (ed.), Encyclopedia of Nanoscience and Nanotechnology, American Scientific Publisher, California, 2003.
[7] J.C. Hummelen, B. Knight, J. Pavlovich, R. González, F. Wudl, Science 269 (1995) 1554.
[8] T. Guo, C.M. Jin, R.E. Smalley, J. Phys. Chem. 95 (1991) 4948.
[9] L. Hultman, S. Stafström, Z. Czigány, J. Neidhardt, N. Hellgren, I.F. Brunell, K. Suenaga, C. Cooliex, Phys. Rev. Lett. 87 (2001) 225503.
[10] S. Stafström, L. Hultman, N. Hellgren, Chem. Phys. Lett. 340 (2001) 227.
[11] R.H. Xie, G.W. Bryant, V.H. Smith Jr., Chem. Phys. Lett. 368 (2003) 486.
[12] M.R. Mana, D.W. Sprehn, H.A. Ichord, J. Am. Chem. Soc. 124 (2002) 13990.
[13] R.H. Xie, G.W. Bryant, J. Zhao, V.H. Smith Jr, A. Di Carlo, A. Pecchia, Phys. Rev. Lett., 90 (2003) 206602.
[14] M.J. Frisch et al., GAUSSIAN 98, Revision A.9, Gaussian, Inc., Pittsburgh, PA, 1998.
[15] A.D. Becke, J. Chem. Phys. 98 (1993) 5648.
[16] J.C. Slater, Phys. Rev. 81 (1951) 385.
[17] A.D. Becke, Phys. Rev. A 38 (1988) 3088.
[18] S.H. Vosko, L. Wilk, M. Nusair, Can. J. Phys. 58 (1980) 1200.
[19] C. Lee, W. Yang, R.G. Parr, Phys. Rev. B 37 (1988) 785.
[20] H.B. Bürgi, E. Blanc, D. Schwarzenbach, S. Liu, Y. Lu, M.M. Kappes, J.A. Ibers, Angew. Chem. Int. Ed. Engl. 41 (1992) 640.
[21] A. Szabo, N.S. Ostlund, Modern Quantum Chemistry, Macmillan, New York, 1982.
[22] ADF 2002.01., Theoretical Chemistry, Vrije Universiteit, Amsterdam, 2002.
[23] G. te Velde, F.M. Bickelhaupt, E.J. Baerends, C. Fonseca Guerra, S.J.A. van Gisbergen, J.G. Snijders, T. Ziegler, J. Comput. Chem. 22 (2001) 931.
[24] R.H. Xie, G.W. Bryant, L. Jensen, J. Zhao, V.H. Smith Jr., J. Chem. Phys. 118 (2003) 8621.
[25] G.D. Zeiss, W.R. Scott, N. Suzuki, D.P. Chong, Mol. Phys. 37 (1979) 1543.
[26] L. Jensen, P.Th. van Duijnen, J.G. Snijders, D.P. Chong, Chem. Phys. Lett. 359 (2002) 524.
[27] D.J. Tozer, N.C. Handy, J. Chem. Phys. 109 (1998) 10180.
[28] S.J.A. van Gisbergen, J.G. Snijders, E.J. Baerends, Phys. Rev. Lett. 78 (1997) 3097.
[29] S.J.A. van Gisbergen, J.G. Snijders, E.J. Baerends, Comput. Phys. Commun. 118 (1999) 119.
[30] W. Krätschmer, K. Fostiropoulos, D.R. Huffman, Chem. Phys. Lett. 170 (1990) 167.
[31] K. Lynch, C. Tanke, F. Menzel, W. Brockner, P. Scharff, E. Stumpp, J. Phys. Chem. 99 (1995) 7985.
[32] J. Onoe, K. Takeuchi, Phys. Rev. B 54 (1996) 6167.
[33] J.R. Cheeseman, M.J. Frisch, G.W. Trucks, T.A. Keith, J. Chem. Phys. 104 (1996) 5497.
[34] R. Taylor, J.P. Hare, A.K. Adul-Sada, H.W. Kroto, J. Chem. Soc. Chem. Commun. 66 (1990) 1423.